JOURNAL OF NANOMATERIALS AND APPLICATIONS

Journal of Nanomaterials and Applications

Journal homepage: https://jna.com.vn

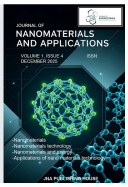

Influence of initial pH on the ultrasonic synthesis of nanosilica from liquid glass

Ştefan Ţălu [1], Hoang Thi Phuong [2,*], Dung Nguyen Trong [3]

[1,] Technical University of Cluj-Napoca, The Directorate of Research, Development and Innovation Management (DMCDI), 15 Constantin Daicoviciu St., Cluj-Napoca, 400020, Cluj county, Romania.

[2, 3,] University of Transport Technology, Faculty of Applied Science, 54 Trieu Khuc, Thanh Xuan, Hanoi, 100000, Vietnam.

Article info

Type of articles:

Original research paper

Corresponding author*:

Hoang Thi Phuong

E-mail address:

bhtanh2@gmail.com

Received: 26 September 2025

Revised: 13 November 2025

Accepted: 15 November 2025

Published: 1 December 2025

Abstract: This study investigates the influence of initial pH on the formation and particle size of nanosilica synthesized from liquid glass (LG) via an ultrasonic assisted method. Nanosilica samples were prepared at pH values of 1, 2, 4, and 6, while maintaining a constant precursor-to-solvent ratio (LG/H_2O=1:2), ultrasonic power of 30 W, sonication time of 15 min, and stirring speed of 500 rpm. Field Emission Scanning Electron Microscopy (FESEM) and particle size distribution analyses revealed a broad particle size range from 15 nm to 400 nm. At pH=2, relatively small particles with a narrow size distribution (~15–20 nm) were obtained, whereas higher pH values (4 and 6) yielded larger particles ranging from 100 to 400 nm. At pH=1, pronounced agglomeration led to irregular particle clusters. These observations were interpreted in terms of the hydrolysis and condensation equilibria of polysilicates under acidic conditions, as well as the steady-state energy dynamics governing particle formation. The findings indicate that pH=2 represents the optimal condition for synthesizing nanosilica from LG, offering a controlled approach to tailoring particle morphology and size. The synthesized nanosilica demonstrates potential applicability in the adsorption of oil-contaminated wastewater.

Keywords: Liquid glass precursors; nanosilica; particle size; polysilicate condensation; ultrasound methods

1. Introduction

Nanosilica has attracted considerable attention across diverse fields, including catalysis, adsorption, biomedicine, and environmental remediation, owing to its high specific surface area, chemical stability, and versatile surface functionalization potential. Various synthesis methods have been reported, such as sol–gel, solution precipitation, hydrothermal techniques, and approaches employing liquid glass precursors (LGP). Among these, the use of LGP is particularly valued due to its cost effectiveness, availability of raw materials, and straightforward synthesis procedure [1]. Historically, the Sol gel method was among the first techniques to employ pH adjustment for controlling particle size. The potential of hydrogen (pH) of the reaction medium has been recognized as a critical factor influencing the formation and morphological characteristics of nanosilica. The equilibrium between polysilicate species such as $Si(OH)_4$, $SiO(OH)_3^-$, and $SiO_2(OH)_2^{2-}$ is strongly dependent on pH, which in turn governs the condensation mechanism and the energetic requirements of particle formation. Some studies reported that a hydroxyl group concentration in the range of 4.9–10 $mmol \cdot g^{-1}$ minimizes the particle formation energy (~25 $kcal \cdot mol^{-1}$), whereas values outside this range substantially increase the energy barrier. Accordingly, initial pH adjustment represents an effective strategy to control nanosilica particle size [2, 3]. The research results showed the influence of pH concentration on the surface charge of nanosilica by simulation method. In the present study, the influence of initial pH on the formation and particle size of nanosilica was systematically investigated. Nanosilica samples were synthesized from LGP under ultrasonic conditions at pH values of 1, 2, 4, and 6. The results indicated that acidic conditions significantly affect the particle formation mechanism. Morphology and particle size were characterized using Field Emission Scanning Electron Microscopy (FESEM) in combination with laser scattering analysis [4]. Recently, several studies have successfully investigated the effects of factors such as temperature and pressure on the structure and phase transition of SiO_2 [5], when doped with Mg to form $MgSiO_3$ [6], Mg_2SiO_4 [7, 8]. With this study, the focus is on the study of the effect of pH concentration on the ultrasonic synthesis of nanosilica from liquid glass. The new point of this article is that the use of ultrasonic energy reduces the synthesis time to 15 minutes, which the traditional sol gel methods have not achieved before. These findings provide deeper insight into the formation mechanism of nanosilica under acidic conditions and identify the optimal pH for controlled synthesis.

2. Materials and methods

2.1. Chemicals and precursors

Liquid glass (LG, sodium silicate solution) was employed as the silica precursor, while distilled water served as the solvent. A dilute sulfuric acid (H_2SO_4) solution was utilized to adjust the pH of the reaction medium. All reagents were of analytical grade and used without further purification.

2.2. Synthesis of nanosilica

Nanosilica was synthesized via an ultrasonic-assisted approach in an acidic medium to investigate the influence of initial pH on particle formation and morphology. The liquid glass precursor (LGP) to water ratio was maintained at 1:2, consistent with the conditions established for the reference standard sample M_3. The initial pH of the reaction medium was systematically adjusted to values of 1, 2, 4 and 6, with the resulting nanosilica samples designated as M_1, M_2, M_3, and M_4, respectively (Table 1). The pH values of 1, 2, 4, and 6 were selected to investigate the distinct effects of decreases pH and weakly acidic environments on particle formation, rather than focusing on intermediate values like pH=3 or 5. The

change pH concentration is the parameter that determines the hydrolysis and condensation mechanism of polysilicate ions. Changing the pH concentration changes the particle size and morphology effectively and cheaply. All other experimental parameters were held constant to ensure reproducibility and isolate the effect of pH. Ultrasonic power was fixed at 30 W, sonication duration at 15 minutes, and mechanical stirring at 500 rpm. This controlled synthesis protocol enabled a comprehensive evaluation of the relationship between acidic conditions and nanosilica particle characteristics, including size distribution and morphological features.

2.3. Analysis and characterization of samples

The synthesized nanosilica samples were subjected to a set of analytical techniques to evaluate their morphological, structural, and particle size characteristics. Prior to characterization, all samples were thoroughly washed with distilled water to remove residual reactants and by-products, followed by drying under controlled conditions to preserve their structural integrity.

2.3.1. Morphological analysis

The surface morphology and microstructural features of the nanosilica particles were examined using FESEM (JEOL, Japan). This technique provided high-resolution imaging, enabling detailed observation of particle shape, surface texture, and the degree of agglomeration. Morphological comparisons across samples allowed for the assessment of how reaction conditions, particularly the initial pH of the medium, influenced particle formation and clustering behavior.

2.3.2. Particle size distribution

Quantitative analysis of particle size and distribution was performed using laser diffraction (Laser Diffraction Particle Size Analyzer). This method facilitated precise measurement of particle size ranges, determination of polydispersity, and evaluation of the uniformity of nanosilica populations. Data from laser diffraction complemented the FESEM observations, providing a correct understanding of both the nanoscale morphology and the statistical distribution of particle dimensions.

2.3.3. Effect of initial pH

The impact of initial pH on nanosilica synthesis was investigated by comparing the morphology, particle size distribution, and agglomeration levels among the samples synthesized at pH =1, 2, 4, and 6 (designated as M_1–M_4). Observed variations in particle size, shape, and clustering were interpreted in terms of the hydrolysis and condensation equilibria of polysilicate species under acidic conditions. These analyses elucidated the role of pH in controlling nucleation, growth, and energy dynamics during particle formation, allowing the identification of optimal conditions for producing nanosilica with controlled morphology and size distribution suitable for targeted applications such as adsorption or catalysis.

3. Results and discussion

3.1. Effect of pH on nanosilica particle size

In this section, the influence of the initial potential of hydrogen (pH) on the formation and morphological characteristics of nanosilica particles was investigated. The synthesized samples are denoted according to the designations provided in Table 1. Representative FESEM images of nanosilica prepared from the LGP at pH values of 1, 2, 4, and 6 are shown in Figures 1–4, respectively, illustrating the effect of acidic conditions on particle size, shape, and aggregation behavior. The LGP to water ratio was maintained at 1:2, consistent with the reference sample M_3, while other experimental parameters including ultrasonic power, sonication time, and stirring speed were kept constant, as established in the precursor-to-solvent ratio study shown in Table 1.

Analysis of the FESEM images revealed the formation of nanosilica particles exhibiting a wide range of sizes, consistent with the laser diffraction results. The particle size distribution spanned approximately 20–400 nm, with samples M_3 and M_4 (synthesized at pH 4 and 6, respectively) displaying relatively larger particles predominantly in the range of 100–400 nm. Remarkably, when nanosilica was synthesized at pH 2 (sample M_2, prepared under identical conditions to the reference sample M_3), a pronounced reduction in particle size was observed, with FESEM images indicating a uniform particle diameter of approximately 15–20 nm. Conversely, in sample M_1 (pH=1, Figure 4), a substantial increase in particle size was detected, accompanied by pronounced agglomeration, reflecting the aggregation of individual silica particles into larger clusters [9].

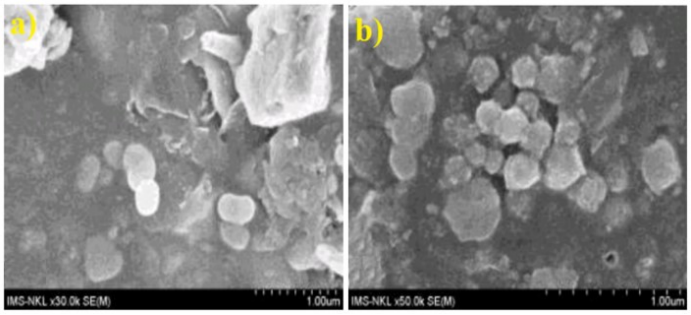

Figure 1. FESEM image of nanosilica LGP sample (sample M_1)

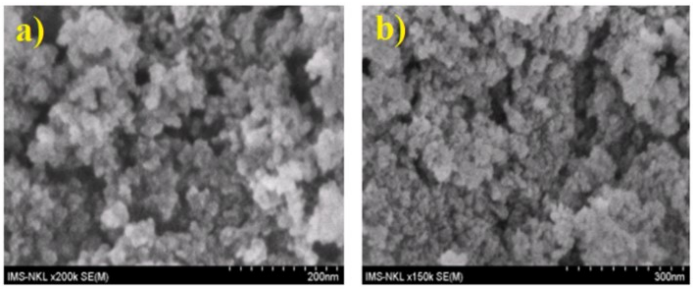

Figure 2. FESEM image of nanosilica LGP sample (sample M_2)

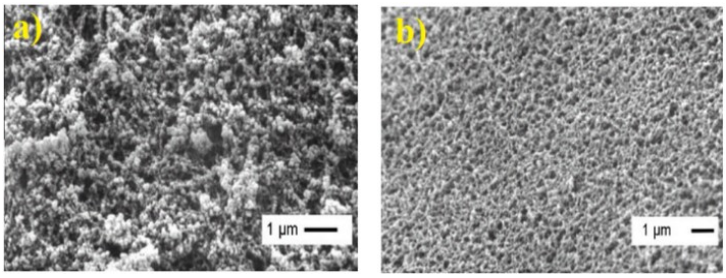

Figure 3. FESEM image of nanosilica LGP sample (sample M_3)

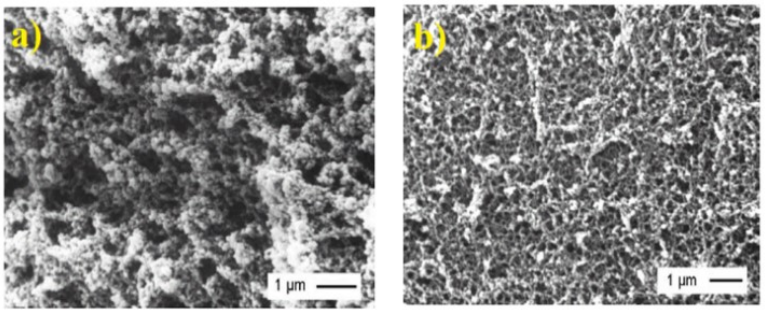

Figure 4. FESEM image of nanosilica LGP sample (Sample M_4)

These observations underscore that an initial pH of 2 provides the most favorable conditions for the controlled synthesis of nanosilica under the employed ultrasonic-assisted methodology. The mechanistic basis for this behavior can be attributed to the acid-mediated hydrolysis and condensation equilibria of polysilicate anions, which predominantly exist in the condensation forms of $Si(OH)_4$, $SiO(OH)_3^-$, and $SiO_2(OH)_2^{2-}$.

Table 1. Synthesis conditions of nanosilica LGP at different pH values

Parameter	M_1	M_2	M_3	M_4
LGP/H_2O	1:2	1:2	1:2	1:2
pH	1	2	4	6
Ultrasonic power [W]	30	30	30	30
Ultrasonic time [min]	15	15	15	15
Stirring speed [rpm]	500	500	500	500

The relative abundances of these species are highly sensitive to the pH of the medium, thereby influencing both nucleation and growth dynamics of nanosilica particles. Previous studies [2, 3] have demonstrated that the concentration of hydroxyl groups associated with different polysilicate moieties critically affects the energetic stability of nanosilica formation. Specifically, when OH^- concentrations are maintained within the range of 4.9–10 mmol·g^{-1}, nanosilica formation occurs at a minimum energy threshold of approximately 25 kcal·mol^{-1}. Deviations outside this range either below 4.9 mmol·g^{-1} or above 10 mmol·g^{-1} result in significantly higher energy requirements for particle formation [9–11]. These findings highlight the necessity of precise pH control to facilitate nanosilica formation under energetically favorable conditions. The structural representation of the liquid glass precursor (LGP) is depicted in Figure 5.

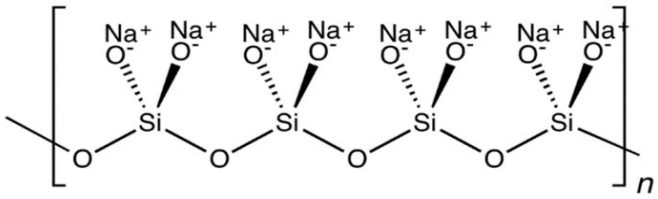

Figure 5. Structure of LGP

At excessively low pH values, polysilicate macromolecules undergo hydrolysis, converting primarily into uncharged poly-$Si(OH)_4$, which limits the condensation necessary for nanoscale particle formation, leading instead to the precipitation of polysilicic acid colloids. In contrast, at excessively high pH values, the generation of a large number of polysilicate radicals promotes uncontrolled aggregation, resulting in an increase in particle size and irregular morphology. Collectively, these mechanistic insights explain the observed trends in particle size and agglomeration, confirming that a moderately acidic environment, specifically pH = 2 with sample M_2, is optimal for the synthesis of uniform, nanoscale silica particles under the ultrasonic-assisted conditions employed in this study.

3.2. Key characteristics of optimally synthesized nanosilica

The particle size distribution of the synthesized nanosilica was quantitatively analyzed using laser diffraction, revealing that the majority of particles were concentrated within the narrow range of 15–25 nm (Figure 6). This low degree of size dispersion indicates a high level of uniformity within the material system, which is a critical attribute for enhancing surface properties and broadening the potential

application spectrum of nanosilica, including adsorption, catalysis, and composite material fabrication. The observed uniformity can be directly correlated with the ultrasonic-assisted synthesis process. The application of ultrasonic waves effectively minimized particle agglomeration, fragmented larger clusters, and facilitated the formation of stable, discrete nanosilica particles.

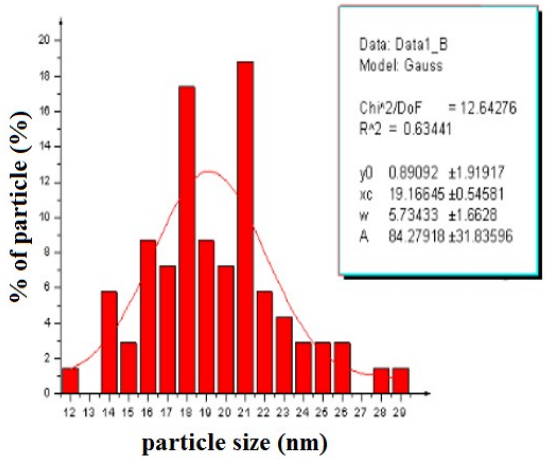

Figure 6. Particle size distribution of nanosilica synthesized from LGP, determined by laser scattering

This cavitation-driven mechanism promotes rapid nucleation and controlled growth, ensuring homogeneity in particle size. Consequently, the ultrasonic treatment not only governs the average particle size but also critically influences the distribution profile, enabling precise control over nanosilica morphology. These results underscore the importance of ultrasonic-assisted processing in tailoring nanosilica characteristics. The synergy between controlled pH conditions and ultrasonic energy input establishes an optimized environment for the formation of highly uniform nanosilica particles, demonstrating that both parameters are interdependent and must be carefully regulated to achieve desired structural and functional properties. Figure 7 shows the X-ray diffraction (XRD) pattern of the synthesized nanosilica, which indicates that the material predominantly exists in an amorphous state [12].

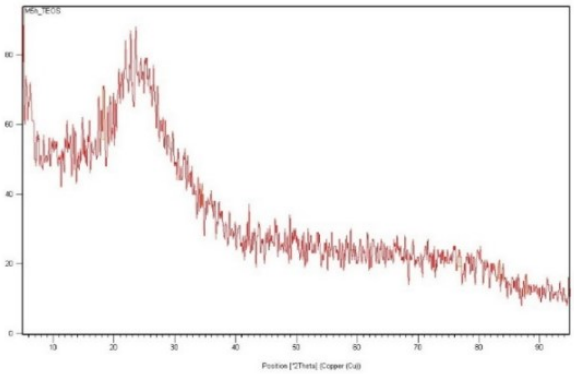

Figure 7. X-ray diffraction pattern of nanosilica synthesized from LGP

The specific surface area, determined using the Brunauer Emmett Teller (BET) method, was measured at 269.8 $m^2 \cdot g^{-1}$. Although this value is moderate compared to other nanostructured silica materials reported in the literature [13–15], it is consistent with the morphological observations obtained from FESEM. Despite the nanoscale particle size, the particles exhibited a tendency to form agglomerated clusters, which decreased their effective dispersion and partially reduced the measured BET surface area.

This behavior can be rationalized based on the particle formation mechanism from LGP, whereby polysilicate chains are progressively fragmented from macromolecules into smaller nanosilica particles. The clustering observed is therefore an intrinsic consequence of the condensation and aggregation processes occurring during ultrasonic-assisted synthesis. Nevertheless, this agglomeration phenomenon can be substantially mitigated by modifying the nanosilica synthesis approach. Specifically, initiating the process from molecular-scale precursors and promoting controlled condensation to form larger particles, while maintaining dimensions within the nanometer range, can improve particle dispersion and uniformity [16]. The N_2 adsorption–desorption isotherm of the nanosilica synthesized from LGP is presented in Figure 8, and the corresponding pore structure parameters are summarized in Table 2. The isotherm exhibits a characteristic hysteresis loop, indicative of capillary condensation within mesoporous structures, consistent with IUPAC type IV classification. Notably, the observed hysteresis loop is relatively narrow and displays a steep adsorption branch within the relative pressure range of P/P_0=0.8–1.0, suggesting the presence of mesoporous capillaries with comparatively large pore dimensions. Quantitative analysis further indicated that the mesoporous capillaries are predominantly centered around ~15 nm, approaching the threshold for large mesopores (>20 nm) [17]. These results corroborate the structural observations from FESEM, demonstrating that although the nanosilica particles are small, they tend to aggregate into clusters, forming mesoporous networks with relatively large pores. This insight highlights the importance of controlling both particle nucleation and condensation dynamics during synthesis to optimize the pore architecture and surface properties for potential applications in adsorption, catalysis, and composite material fabrication.

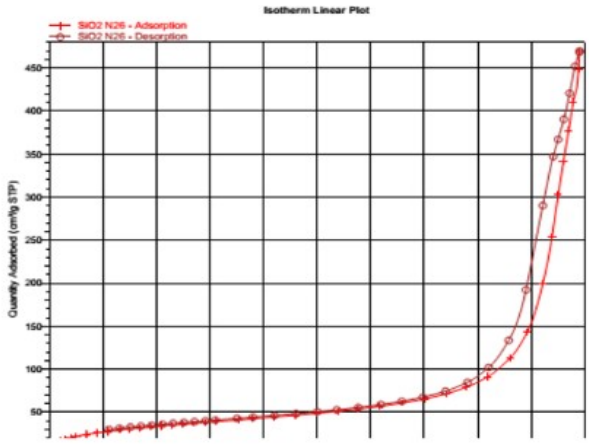

Figure 8. N_2 adsorption–desorption isotherm of nanosilica synthesized from LGP

Table 2. Porous properties of nanosilica LGP materials

Model	S_{BET} [$m^2 \cdot g^{-1}$]	V_{meso} [$cm^3 \cdot g^{-1}$]	D_{meso} [nm]
M_2	269.8	1.16759	15.859

3.3. Adsorption performance of nanosilica LGP for Bach Ho crude oil under simulated seawater conditions

The adsorption performance of the nanosilica LGP sample (M_2) was evaluated for Bach Ho crude oil in a simulated seawater environment, prepared as a 3.5‰ NaCl solution, corresponding to the typical salinity of natural seawater. Representative adsorption images, presented in Figure 9, indicate that the nanosilica particles effectively interacted with the crude oil, demonstrating promising preliminary

adsorption behavior.

The calculated adsorption capacity of the sample was determined to be 2.9g of crude oil per gram of nanosilica. Although this result reflects significant adsorption, indicates substantial adsorption potential, though further optimization could enhance performance. The limited performance can be attributed primarily to the pronounced aggregation of nanosilica particles, which reduces dispersion and consequently diminishes the effective specific surface area available for adsorption [18]. Additionally, the as-synthesized nanosilica particles exhibited limited hydrophobicity, which further limits their interaction with the hydrophobic crude oil phase. These findings highlight the potential of LGP derived nanosilica for oil adsorption while indicating the need for further surface modification and optimization to enhance efficiency.

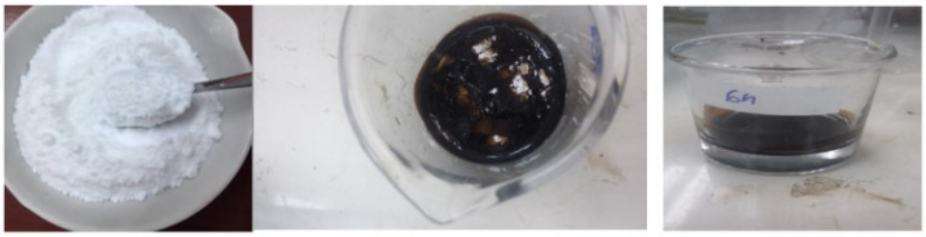

Figure 9. Experimental observation of crude oil adsorption by nanosilica LGP (sample M_2)

4. Conclusion

This study investigated the effect of the initial pH on the synthesis of nanosilica from LGP under ultrasonic-assisted conditions. Experimental results demonstrated that the pH of the reaction medium plays a decisive role in governing particle nucleation, growth, and aggregation behavior. At an optimal value of pH=2, nanosilica with a narrow particle size distribution in the range of 15–25 nm was obtained, exhibiting uniform morphology and reduced agglomeration compared to other tested conditions. In contrast, at pH=4–6, the formation of significantly larger particles (100–400 nm) was observed, while at pH=1, strong aggregation dominated, leading to irregular clusters and diminished control over the particle formation process. Structural characterization confirmed that the synthesized nanosilica primarily exists in an amorphous state, as evidenced by XRD analysis. BET measurements further revealed a specific surface area of 269.8 $m^2 \cdot g^{-1}$ and an average mesopore diameter of ~15nm, corresponding to the mesoporous regime. The pore size distribution and surface area values are consistent with the FESEM observations, where small primary nanoparticles tend to form aggregates, thus partially reducing the accessible surface area. Preliminary evaluation of the environmental application potential showed that the nanosilica LGP material (sample M_2) exhibits the capacity to adsorb 2.9g of Bach Ho crude oil per gram of nanosilica in a simulated seawater medium (3.5‰ NaCl solution). While this result highlights the promising oil adsorption potential of nanosilica, the performance has not yet reached its theoretical maximum. The reduced efficiency can be attributed to particle agglomeration and insufficient hydrophobic surface characteristics of the as-prepared nanosilica. Taken together, these findings establish pH=2 as the most favorable condition for nanosilica synthesis from LGP under ultrasonic treatment, offering control over particle size and morphology. Furthermore, the obtained nanosilica materials demonstrate potential for application in oil spill remediation and environmental treatment technologies. Future work should focus on surface functionalization and hydrophobic modification strategies to enhance dispersion stability and adsorption efficiency, thereby improving the applicability of LGP derived nanosilica in large-scale environmental remediation processes.

Funding: The work received no funding.

Data Availability Statement: The data that support the findings of this study are available from the corresponding author upon reasonable request.

Competing interests: The authors declare that they have no competing interests.

References

[1] W. Stöber, A. Fink, E. Bohn. (1968). Controlled growth of monodisperse silica spheres in the micron size range. Journal of Colloid and Interface Science, 26(1), 62–69. https://doi.org/10.1016/0021-9797(68)90272-5.

[2] N. Nazemzadeh, C.R. Miranda, Y. Liang, M.P. Andersson. (2023). First-principles prediction of amorphous silica nanoparticle surface charge: Effect of size, pH, and ionic strength. Journal of Physical Chemistry Part B: Condensed Matter, Materials, Surfaces, Interfaces & Biophysical, 127, 9608–9619. https://doi.org/10.1021/acs.jpcb.3c04405.

[3] D. Napierska, et al. (2010). The nanosilica hazard: another variable entity. Particle and Fibre Toxicology, 7, 39. http://www.particleandfibre toxicology. com/content/7/1/39.

[4] T.Y. Yee, M.O. Fatehah. (2017). Characterization and transformation of silicon dioxide nanoparticles. International Journal of Environmental Engineering, 8(4), 143–150. Doi: 10.5829/ijee.2017.08.04.03.

[5] D.N. Trong, V.C. Long, Ş. Ţălu, U. Saraç, P.N. Dang and K.P. Huu, (2022), A New Study on the Structure, and Phase Transition Temperature of Bulk Silicate Materials by Simulation Method of Molecular Dynamics, *J. Compos. Sci. 6*(8), 234, https://doi.org/10.3390/jcs6080234

[6] T.T. Quoc, D.N. Trong, (2019) Molecular dynamics studies the effects of the earth's surface depth on the heterogeneous kinetics of $MgSiO_3$, Results in Physics, 15, 102671.
https://doi.org/10.1016/j.rinp.2019.102671

[7] D.N. Trong, T.T. Quoc, Ş. Ţălu, (2025), Impact of High Temperature and Pressure on the Structure and Phase Transition of Mg_2SiO_4 Oxide via Molecular Dynamics Simulation, Physica B: Condensed Matter, 717, 417784. https://doi.org/10.1016/j.physb.2025.417784.

[8] T.T. Quoc, D.N. Trong, V.C. Long, K.P. Huu, Ş. Ţălu, (2024), Effects of liquefied gas temperature and negative pressure on the microstructural characteristics of oxide Mg_2SiO_4 using molecular dynamics simulation method, Computational Materials Science, 242, 113075.
https://doi.org/10.1016/j.commatsci.2024.113075

[9] D. Makimura, C. Metin, T. Kabashima, T. Matsuoka, Q.P. Nguyen, C.R. Miranda. (2010). Combined modeling and experimental studies of hydroxylated silica nanoparticles. Journal of Materials Science, 45(18), 5084–5088. https://doi.org/10.1007/s10853-010-4390-y

[10] F. Caldelas, M.J. Murphy, C. Huh, S.L. Bryant. (2011). Factors governing distance of nanoparticle propagation in porous media. OnePetro (SPE Papers), Paper SPE 142305-MS.
https://doi.org/10.2118/142305-MS

[11] H. Reiber, T. Köller, T. Palberg, F. Carrique, E.R. Reina, R. Piazza. (2007). Salt concentration and particle density dependence of electrophoretic mobilities of spherical colloids in aqueous suspension. Journal of Colloid and Interface Science, 309(2), 315–322. https://doi.org/10.1016/j.jcis.2007.01.006.

[12] D.Q. Yang, J.N. Gillet, M. Meunier, E. Sacher. (2005). Room temperature oxidation kinetics of Si nanoparticles in air, determined by x-ray photoelectron spectroscopy. Journal of Applied Physics, 97,

024303. https://doi.org/10.1063/1.1835566.
[13] K.L. Wang. (2010). Research of improving water injection effect by using active SiO_2 nano-powder in the low-permeability oilfield. Advanced Materials Research, 92, 207–212.
https://doi.org/10.4028/www.scientific.net/AMR.92.207
[14] P. Nikolaos, V. Emmanouil, N.P. Harilaos, T. George. (2004). A high-level synthesis of oil spill response equipment and countermeasures. Journal of Hazardous Materials, 107, 51–58.
https://doi.org/10.1016/j.jhazmat.2003.11.009.
[15] S.X. Xie, G.C. Jiang, M. Chen, Z.Y. Li, X.B. Huang, C. Liang. (2014). Harmless treatment technology of waste oil–based drilling fluids. Energy Sources, Part A: Recovery, Utilization, and Environmental Effects, 36(9), 1043–1049. https://doi.org/10.1080/10916466.2011.638691.
[16] V.L. Alexeev, P. Ilekti, J. Persello, sJ. Lambard, T. Gulik, B. Cabane. (1996). Dispersions of silica particles in surfactant phases. Langmuir, 12, 2392–2401. https://doi.org/10.1021/la950707c.
[17] A. Lazaro, M.C. Van de Griend, H.J.H. Brouwers, J.W. Geus. (2013). The influence of process conditions and Ostwald ripening on the specific surface area of olivine nano-silica. Microporous and Mesoporous Materials, 181, 254–261. https://doi.org/10.1016/j.micromeso.2013.08.006.
[18] Ș. Țălu. (2015). Micro and nanoscale characterization of three-dimensional surfaces: Basics and applications. Napoca Star Publishing House, Cluj-Napoca, Romania. ISBN: 978-606-690-349-3.